



Published in final edited form as:

*J Biomech.* 2018 June 06; 74: 32–40. doi:10.1016/j.jbiomech.2018.04.013.

## Sun-mediated Mechanical LINC between Nucleus and Cytoskeleton Regulates $\beta$ catenin Nuclear Access

Gunes Uzer<sup>\*,1,2</sup>, Guniz Bas<sup>1</sup>, Buer Sen<sup>2</sup>, Zhihui Xie<sup>2</sup>, Scott Birks<sup>1</sup>, Melis Olcum<sup>2</sup>, Cody McGrath<sup>2</sup>, Maya Styner<sup>2</sup>, and Janet Rubin<sup>2</sup>

<sup>1</sup>Boise State University

<sup>2</sup>University of North Carolina Chapel Hill

### Abstract

$\beta$ catenin acts as a primary intracellular signal transducer for mechanical and Wnt signaling pathways to control cell function and fate. Regulation of  $\beta$ catenin in the cytoplasm has been well studied but  $\beta$ catenin nuclear trafficking and function remains unclear. In a previous study we showed that, in mesenchymal stem cells (MSC), mechanical blockade of adipogenesis relied on inhibition of  $\beta$ catenin destruction complex element GSK3 $\beta$  (glycogen synthase kinase 3 $\beta$ ) to increase nuclear  $\beta$ catenin as well as the function of Linker of Cytoskeleton and Nucleoskeleton (LINC) complexes, suggesting that these two mechanisms may be linked. Here we show that shortly after inactivation of GSK3 $\beta$  due to either low intensity vibration (LIV), substrate strain or pharmacologic inhibition,  $\beta$ catenin associates with the nucleoskeleton, defined as the insoluble nuclear fraction that provides structure to the integrated nuclear envelope, nuclear lamina and chromatin. Co-depleting LINC elements Sun-1 and Sun-2 interfered with both nucleoskeletal association and nuclear entry of  $\beta$ catenin, resulting in decreased nuclear  $\beta$ catenin levels. Our findings reveal that the insoluble structural nucleoskeleton actively participates in  $\beta$ catenin dynamics. As the cytoskeleton transmits applied mechanical force to the nuclear surface to influence the nucleoskeleton and its LINC mediated interaction, our results suggest a pathway by which LINC mediated connectivity may play a role in signaling pathways that depend on nuclear access of  $\beta$ catenin.

---

**Corresponding author:** Gunes Uzer PhD, Boise State University, Department of Mechanical & Biomedical Engineering, 1910 University Drive, MS-2085, Boise, ID 83725-2085, Ph. (208) 426-4461, gunesuzer@boisestate.edu.

**Publisher's Disclaimer:** This is a PDF file of an unedited manuscript that has been accepted for publication. As a service to our customers we are providing this early version of the manuscript. The manuscript will undergo copyediting, typesetting, and review of the resulting proof before it is published in its final citable form. Please note that during the production process errors may be discovered which could affect the content, and all legal disclaimers that apply to the journal pertain.

#### Author Contributions

**Gunes Uzer** concept/design, data analysis/interpretation, financial support, manuscript writing, final approval of manuscript

**Guniz Bas** data analysis, final approval of manuscript

**Buer Sen** data analysis, final approval of manuscript

**Zhihui Xie** data analysis, final approval of manuscript

**Scott Birks** data analysis, final approval of manuscript

**Melis Olcum** final approval of manuscript

**Cody McGrath** final approval of manuscript

**Maya Styner** final approval of manuscript

**Janet Rubin** concept/design, financial support, data analysis/interpretation, manuscript writing, final approval of manuscript

The author(s) declare no competing financial interests.

## Keywords

Sun; Nesprin; Lamin; LINC; Nucleoskeleton; Nuclear Envelope;  $\beta$ catenin; Bone; Adipogenesis; Mechanical Signals; Mesenchymal Stem Cells

---

## Introduction

Mechanical forces acting within the cellular environment define cellular form, and drive physiological function.  $\beta$ catenin, the primary effector molecule of Wnt signaling axis (Baron and Kneissel, 2013) is central to mechanosignaling and its mechanical activation is a part of normal physiologic response (Robinson et al., 2006). In the case of musculoskeletal progenitor mesenchymal stem cells (MSC), mechanical signals generated during loading promote osteoblast differentiation (Uzer et al., 2013) and inhibit adipocyte recruitment (Sen et al., 2011). These MSC phenotypes are in part controlled by mechanically and chemically regulated  $\beta$ catenin signaling (Sen et al., 2008). How  $\beta$ catenin moves from cytoplasm into the nucleus after stimulation is unclear. At the cellular level, forces imposed on the cytoskeleton not only activate signaling events but promote cytoskeletal structure configurations that enhance activation of mechanosignaling pathways (Burrige and Wittchen, 2013; Uzer et al., 2016). In this way, cytoskeletal structure and connectivity may play a direct role in  $\beta$ catenin nuclear trafficking.

$\beta$ catenin control of gene expression relies on its nuclear localization (Cong et al., 2003), but it does not possess a classic nuclear localization signal; instead,  $\beta$ catenin's armadillo repeat sequence is believed to mediate nuclear transit through direct contact with the nuclear pore complex (NPC) (Koike et al., 2004; Tolwinski and Wieschaus, 2004). NPCs bind to nuclear lamina at the inner nuclear envelope, a highly organized structure that maintains dynamic connectivity with both chromatin and cytoplasmic cytoskeleton (Gruenbaum et al., 2005). In this way, reflecting its functionality in organizing internal structure and external connectivity, the structural component of the nucleus has been referred to as the "nucleoskeleton" (Cook, 1988). The nucleoskeleton acts as a master scaffold for regulatory proteins, transcription factors and chromatin to regulate functions of nuclear machinery (Simon and Wilson, 2011); this suggests that  $\beta$ catenin might utilize the existing nucleoskeletal network to facilitate nuclear entry.

Connectivity between the nucleoskeleton and the cytoplasmic cytoskeleton is maintained by a mechanosensitive complex called LINC (Linker of Nucleoskeleton and Cytoskeleton) (Crisp et al., 2006) which traverses the nuclear envelope. The LINC complex is made up of multiple components: actin binding giant Nesprin Proteins 1&2 which are anchored to the inner nucleus by Sun proteins 1& 2, that finally interact with the inner Lamin A/C network. We have shown that disabling LINC function via siRNA deletion of Sun-1 and Sun-2 proteins, or by overexpressing the Nesprin KASH (Klarsicht, ANC-1, Syne Homology) domain, not only decreases mechanical responsiveness to mechanical challenges but also promotes adipogenesis of MSCs (Uzer et al., 2015), a process largely dependent on nuclear  $\beta$ catenin (Sen et al., 2009).  $\beta$ catenin is known to be retained at cell-cell junctions (Aberle et al., 1996) and recently, KASHless small Nesprin isoforms were shown to cause  $\beta$ catenin

localization to the plasma membrane (Zhang et al., 2016). Reminiscent of the disposition of  $\beta$ catenin at cell-cell contacts at the plasma membrane, the Nesprin component of the LINC complex also associates with  $\beta$ catenin at the nuclear envelope (Lu et al., 2012; Neumann et al., 2010). Consistent with a potential regulatory role of LINC complexes for  $\beta$ catenin, progeroid mutations involving LINC and nucleoskeleton elements (Gruenbaum et al., 2005) are marked by increased adipogenic infiltration in musculoskeletal tissues indicating reductions in Wnt activity and cellular  $\beta$ catenin (Hernandez et al., 2010). As such, the LINC complex may serve as a critical regulator of MSC fate through influencing  $\beta$ catenin trafficking.

Here, utilizing sub-cellular fractionation and immunostaining experiments, we show that both mechanically and biochemically-induced  $\beta$ catenin nuclear entry is preceded by a rapid but transient association of the molecule with the nucleoskeleton. The LINC elements Sun-1 and Sun-2 are critical in facilitating this  $\beta$ catenin-nucleoskeleton interaction. When LINC connectivity is disrupted via Sun-1&2 co-depletion, basal levels of nuclear  $\beta$ catenin drop and its interaction with the nucleoskeleton is impaired. Loss of LINC connectivity thus results in decreased efficiency of both mechanical and biochemical  $\beta$ catenin-activating events.

## Results

### Mechanical inactivation of GSK3 $\beta$ leads to a non-monotonic increase of nuclear $\beta$ catenin

Mechanical strain application activates Focal Adhesion Kinase (FAK) and, through Fyn mediated recruitment of mTORC2 (Thompson et al., 2013), activates Akt (Ser 473). This leads to phosphorylation (Ser 9) and inhibition of GSK3 $\beta$ , preventing  $\beta$ catenin proteolysis (Case et al., 2010). Similar to strain, low intensity vibration (LIV), also activates FAK/Akt, promotes MSC osteogenesis and inhibit adipogenesis (Uzer et al., 2015). Here, using marrow derived MSCs, we tested whether LIV inhibits GSK3 $\beta$ . We probed for Akt and GSK3 $\beta$  phosphorylation immediately following LIV (0.7g, 90Hz, 20min). LIV increased both p-Akt (277%,  $p<0.001$ ) and p-GSK3 $\beta$  (246%,  $p<0.001$ ) consistent with decreased  $\beta$ catenin proteolysis (Fig. 1a). Application of strain (2%, 0.17Hz, 20min) also increased p-Akt (218%,  $p<0.001$ ) and p-GSK3 $\beta$  (181%,  $p<0.001$ ) when compared to non-strained controls (Fig. 1b).

$\beta$ catenin enters the nucleus to activate its gene targets (Cong et al., 2003). We separated the soluble from the insoluble nuclear fraction and probed for localization of active (nonphosphorylated)  $\beta$ catenin via western blot analysis. As indicated in Fig. 1c&d, 180 min after loading both LIV (177%,  $p<0.01$ ) and strain (173%,  $p<0.001$ ) samples showed increased  $\beta$ catenin localization to the soluble nuclear protein fractions. PCR analysis further indicated that both LIV (205%,  $p<0.05$ ) and strain (198%,  $p<0.05$ ) application increased expression of Axin-2 mRNA, a positive transcriptional target of  $\beta$ catenin (Leung et al., 2002).

To better understand  $\beta$ catenin localization prior to nuclear entry, we probed nuclear  $\beta$ catenin levels both immediately and 120 min after a single application of LIV or strain. Similar to our findings at 180 min post-load, we found increased  $\beta$ catenin levels in the soluble nuclear

fraction 120 min post-LIV (Fig. 1e, 140%,  $p<0.05$ ) and at 120 min post-strain (Fig. 1f, 158%,  $p<0.05$ ). This long-term increase of  $\beta$ catenin in the soluble nuclear fraction was non-monotonic and was preceded by a significant decrease in the soluble nuclear  $\beta$ catenin immediately following both LIV (Fig. 1e, 20 min, 49%,  $p<0.05$ ) and strain (Fig. 1f, 20 min, 45%,  $p<0.05$ ). These findings suggest that assay of the soluble nuclear fraction may reflect only a subset of total nuclear  $\beta$ catenin, and indicate that  $\beta$ catenin interacts with distinct nuclear compartments that are excluded in assays which capture only the soluble nuclear fraction.

### **Mechanical signals cause a rapid and transient $\beta$ catenin association with the nucleoskeleton**

As  $\beta$ catenin lacks a classical nuclear localization signal, it is thought to directly interact with Nuclear Pore Complexes (NPCs) during nuclear entry (Sharma et al., 2012).  $\beta$ catenin forms complexes with LINC component Nesprin at the nuclear envelope (Markiewicz et al., 2006; Neumann et al., 2010) suggesting that the cell cytoskeleton interacts with the LINC complex to provide a scaffold to localize  $\beta$ catenin in close proximity of NPCs. Depicted in Fig. 2a, we tested this possibility by extracting the insoluble nucleoskeletal (Nsk) fraction. The Nsk fraction was found to be free of the soluble nuclear protein marker PARP, but rich in the nuclear envelope proteins, Sun-1, Sun-2, Nesprin-1, as well as structural proteins LaminA/C and nucleoporin Nup358. Emerin was found in both soluble and insoluble fractions. We probed for a  $\beta$ catenin-Nsk interaction immediately following the application of either LIV (0.7g, 90Hz, 20min) or strain (2%, 0.17Hz, 20min), times when  $\beta$ catenin levels in the soluble nuclear fraction were decreased; LaminA/C was used as a referent. Immediately after LIV, the  $\beta$ catenin-Nsk association was increased to  $179\pm 8.4\%$  that of control cells (Fig. 2b,  $p<0.05$ ). Application of strain similarly increased  $\beta$ catenin-Nsk association to  $189\pm 17\%$  (Fig. 2c,  $p<0.05$ ).

Akt signal activation resulting from both LIV and strain is transient, returning to baseline within 120 min (Uzer et al., 2015). We thus tested if the mechanically directed interaction between  $\beta$ catenin and Nsk was also transient: at the 140min time point, the  $\beta$ catenin-Nsk association dropped below baseline ( $82\pm 16\%$ , NS) (Fig. 2b). This drop in the baseline association corresponds to the time when the soluble nuclear  $\beta$ catenin fraction rises (Fig. 1e-f). At this point, if LIV was reapplied,  $\beta$ catenin-Nsk association again rose to  $176\pm 19\%$  of the baseline ( $p<0.05$ ). Similarly, with strain, the stimulated association of  $\beta$ catenin-Nsk returned to baseline levels 120 min after the first strain application ( $73\pm 26\%$ , NS) (Fig. 2c). A second strain bout once again increased the  $\beta$ catenin-Nsk association to  $200\pm 4.3\%$  ( $p<0.05$ ). These findings confirm that  $\beta$ catenin's association with the nucleoskeleton is transient and indicate that mechanically directed association of  $\beta$ catenin with the nucleoskeleton precedes translocation of  $\beta$ catenin into the soluble nuclear fraction.

### **Co-depletion of LINC elements Sun-1 and Sun-2 disrupts $\beta$ catenin traffic into the soluble nuclear fraction**

The mechanically-induced association of  $\beta$ catenin with the nucleoskeleton suggests that nucleo-cytoskeletal connectivity might be necessary for  $\beta$ catenin trafficking. To answer this question, we disabled LINC function in MSCs through siRNA depletion of both Sun-1 and

Sun-2 proteins (siSUN). Cells treated with siSUN showed a 57% ( $p < 0.01$ ) increase in nuclear height to  $7.9 \pm 0.6 \mu\text{m}$ , compared to average height of  $5.0 \pm 0.4 \mu\text{m}$  in siCtrl cells, and a 23% ( $p < 0.05$ ) decrease in nuclear area from  $472.9 \pm 8.8 \mu\text{m}^2$  to  $360.2 \pm 10.4 \mu\text{m}^2$ . Nuclear volume remained the same in both groups (Fig. 3a). Co-depletion of Sun-1 and Sun-2 caused dislocation of the actin-binding element of LINC complex, Nesprin-2, from the nuclear envelope and its dispersal into the ER membranes (Fig. S1b&c), together confirming the loss of cytoskeletal constraints on the nucleus. We did not consider Nesprin-1 as MSCs used in this study do not to express the giant Nesprin-1 known to bind F-actin (Meyer et al., 2016). Our data indicate that loss of Sun-1 and Sun-2 mediated connections reduce the force on the nucleus by untethering Nesprin-2.

We next turned our attention to  $\beta$ catenin localization. Comparing  $\beta$ catenin levels in nucleoskeletal and soluble nuclear fractions, siSUN treatment decreased the  $\beta$ catenin-Nsk association to  $51 \pm 3.7\%$  (Fig. 3b,  $p < 0.001$ ) and nuclear  $\beta$ catenin levels to  $59 \pm 7.8\%$  of controls ( $p < 0.05$ , Fig. 3c). Axin-2 mRNA was decreased to  $72 \pm 3.6\%$  (Fig. 3d,  $p < 0.05$ ), suggesting that  $\beta$ catenin's effect on gene targets was diminished when  $\beta$ catenin was prevented from associating with the nucleoskeleton.

Nesprin has been implicated in the nuclear localization of  $\beta$ catenin. While its exact function in this regard remains unclear, Nesprin forms complexes with  $\beta$ catenin and loss of Nesprin decreases the soluble nuclear level of  $\beta$ catenin (Neumann et al., 2010). We immunoprecipitated Nesprin-2 to confirm its co-localization with  $\beta$ catenin in our MSCs (Fig. S1a) and immunostained for Nesprin-2 and  $\beta$ catenin (Fig. 3e). Immunostaining in LINC deficient MSCs (+ siSUN) showed that Nesprin-2 became untethered from the nuclear surface (Fig. 3e, Fig. S1b&d). To understand whether  $\beta$ catenin followed the same trend after Nesprin-2 dislocation from the nuclear envelope, we quantified Nesprin-2/ $\beta$ catenin co-localization. We found  $\beta$ catenin to be co-localized with Nesprin-2 at the nuclear periphery in siSUN treated MSCs (Fig. 3e). Quantifying the extra-nuclear to intra-nuclear Nesprin-2/ $\beta$ catenin co-localization with respect to nuclear position showed it increased 10-fold in siSUN treated MSCs compared to controls (Fig. 3e, Fig. S1b,  $p < 0.001$ ). This suggests that intact Nesprin-2 positioning localizes  $\beta$ catenin to the nuclear envelope and may provide access to the NPC to facilitate inward transfer. To quantify the rate of  $\beta$ catenin nuclear entry, we measured fluorescence recovery after photo bleaching (FRAP) of nuclear GFP- $\beta$ catenin. Following photo bleaching of nuclear GFP- $\beta$ catenin, siCtrl treated MSCs showed that recovery halftime of GFP- $\beta$ catenin in the nucleus was  $33.7 \pm 3.6$  seconds while siSUN treated cells required 16 seconds longer to recover (Fig. 3f, 48%  $p < 0.05$ ), at  $49.5 \pm 3.4$  seconds. This confirms that replenishment of nuclear  $\beta$ catenin is slowed when the LINC complex is disrupted.

To ascertain whether LINC involvement was critical for non-mechanical activation of  $\beta$ catenin, we inhibited GSK3 $\beta$  with the specific inhibitor, SB415286 ("SB415") which causes nuclear  $\beta$ catenin transfer. Treatment with SB415 resulted in a continuous increase in the soluble nuclear  $\beta$ catenin levels by  $182 \pm 22\%$  ( $p < 0.05$ ) and  $266 \pm 29\%$  ( $p < 0.01$ ) of baseline levels at 120 min and 240 min, respectively (Fig. 4a). This contrasted with the non-monotonic increase accompanying mechanical stimulation. At the 180 min time point, siSUN treatment decreased both basal and SB415 induced levels of nuclear  $\beta$ catenin (Fig.

4b,  $p < 0.05$ ). The  $\beta$ catenin-Nsk association increased to  $165 \pm 27\%$  ( $p < 0.05$ ) in control cells (siCtrl) treated with SB415 at 180 min; this increase was also visible at earlier time points of 20, 140 and 160 minutes (Fig. S2), contrasting to the non-monotonic increase following mechanical challenge. Importantly, siSUN decreased the basal  $\beta$ catenin-Nsk association SB415 treated cells to  $63 \pm 13\%$  of control (Fig. 4c,  $p < 0.05$ ). These findings suggest that LINC complex connectivity with the nucleoskeleton is important for  $\beta$ catenin nuclear entry, whatever the stimulus.

### **LINC elements Sun-1 and Sun-2 are necessary for mechanically-induced $\beta$ catenin nuclear entry**

We next asked if Sun-1 and Sun-2 mediated LINC connectivity was critical for the mechanically-induced transfer of  $\beta$ catenin to the Nsk fraction. Using Sun-1/2 depletion to untether the  $\beta$ catenin-binding element of LINC, Nesprin-2, we found decreased basal Nsk-bound  $\beta$ catenin ( $40 \pm 9\%$ ,  $p < 0.05$ , Fig. 4d). This further inhibited LIV's effect to induce a  $\beta$ catenin-Nsk association (Fig. 4d,  $p < 0.05$ ) while depletion of Emerin or Lamin A/C failed to repress LIV induced  $\beta$ catenin-nucleoskeleton association (Fig. S3a&b). Strain-induced  $\beta$ catenin-Nsk association was also reduced by siSUN treatment (Fig. 4e,  $p < 0.05$ ). Importantly, inhibition of the strain-induced  $\beta$ catenin-Nsk association after siSUN treatment did not affect proximal Akt and GSK3 $\beta$  phosphorylation, but did inhibit accumulation of nuclear  $\beta$ catenin (Fig. S4). To further assess the progressive inward localization of  $\beta$ catenin we tracked its associations with its binding partner Nesprin-2, we immunoprecipitated Nesprin-2 immediately following LIV treatment; the association of Nesprin-2 with  $\beta$ catenin decreased to  $50 \pm 2\%$  (Fig. 4f,  $p < 0.001$ ).

## **Discussion**

$\beta$ catenin is an important signaling molecule in the control of cell fate, and is subject to both mechanical and biochemical activation to induce its translocation into the nucleus (Tolwinski and Wieschaus, 2004).  $\beta$ catenin lacks classical a nuclear localization signal (Koike et al., 2004), rather it appears to directly dock onto nuclear surface before inward transfer through Nuclear Pore Complexes (NPCs). As such, increasing cytoplasmic levels of  $\beta$ catenin via inhibiting GSK3 $\beta$ -dependent proteolysis serves to increase the probability that  $\beta$ catenin is positioned at the nuclear surface. We show here, for the first time, that in addition to mechanical strain, which activates Akt to phosphorylate and inhibit GSK3 $\beta$  (Case et al., 2008), LIV also inactivates GSK3 $\beta$ , resulting in decreased  $\beta$ catenin proteolysis. In this way, both mechanical applications increase  $\beta$ catenin accumulation in the soluble nuclear fraction 3 hours after initiating the specific force. These finding are supportive of our earlier findings that both LIV and strain results in preservation of  $\beta$ catenin activity in mesenchymal stem cells in a dose dependent manner (Sen et al., 2011) and activate common cytoskeletal signaling pathways (Uzer et al., 2015). Consistent with a transient inactivation of GSK3 $\beta$  (Sen et al., 2009), the mechanical increase in nuclear  $\beta$ catenin accumulation is non-monotonic; in fact, measuring nuclear  $\beta$ catenin immediately after LIV or strain showed a significant decrease in nuclear  $\beta$ catenin, suggesting previously unanalyzed interactions with structural components of the nucleus.

Recent high-resolution imaging studies have shown that actin filaments create nuclear indentations where they connect to the nuclear surface at points in close proximity to nuclear pore complexes and chromatin (Jorgens et al., 2016). The NPCs interact with elements of the LINC complex: Giant Nesprin-2, which serves as the actin binding element on the nuclear surface also form complexes with  $\beta$ catenin, and the Nesprin anchoring element Sun-1 (but not its co-element Sun-2) directly interacts with NPCs (Liu et al., 2007). This suggests that LINC complexes could provide an anchor to situate  $\beta$ catenin on the nuclear surface in close proximity to NPCs, thus positioning it for transfer inward. By isolating a nucleoskeletal fraction separate from the internal soluble nuclear component, we found that  $\beta$ catenin interaction with the nucleoskeleton increased immediately after mechanical challenge, an event which precedes the eventual transfer of the signaling molecule into the soluble nuclear fraction. As mechanical challenges (e.g., LIV and strain) induce only a transient activation of  $\beta$ catenin (Sen et al., 2011), it was not surprising that the  $\beta$ catenin-Nsk association was also transient, and returned to baseline levels within 2 hours after mechanical challenge. A second mechanical challenge induced a second wave of  $\beta$ catenin-Nsk association – again preceding nuclear entry, suggesting that the nucleoskeleton provides a critical gate for  $\beta$ catenin to access the nucleus. In the case of pharmacological inhibition of GSK3 $\beta$ , which is not transient but rather continuous,  $\beta$ catenin's association with the nucleoskeleton was persistently elevated during  $\beta$ catenin nuclear accumulation, and as such, the LINC “gate” remained open.

Supporting the hypothesis that association with LINC at the nuclear envelope regulate nuclear  $\beta$ catenin levels, previous studies have shown decreased  $\beta$ catenin levels within the soluble nuclear fraction in Nesprin-2 depleted cells (Neumann et al., 2010). Interestingly, KASHless isoforms of Nesprin also form complexes with  $\beta$ catenin at cell-cell junctions and can regulate  $\beta$ catenin availability in the cytoplasm (Zhang et al., 2016). As Nesprin-2 and Nesprin-1 possess various isoforms (Duong et al., 2014) that could confound studies of giant Nesprin's contribution to LINC mediated events, we used a complimentary method to disrupt LINC associations of co-depleting Sun-1 and Sun-2 proteins (Tajik et al., 2016). We have previously Sun depletion causes Nesprin-2 dislocation from nuclear envelope (Uzer et al., 2015). Further, untethering of the actin cytoskeleton from the nucleus increases mesenchymal stem cell adipogenesis—a process largely controlled by  $\beta$ catenin (Case et al., 2010). Consistent with the loss of LINC-mediated nucleo-cytoskeletal coupling and cellular contractility in Sun-1/2 depleted cells (Graham et al., 2018), co-depletion of Sun-1 and Sun-2 proteins here resulted in nuclei that were rounded. The release of nuclear connection also decreased  $\beta$ catenin levels in the traditional soluble fraction thought to represent the inner nucleus, and diminished transcription of the  $\beta$ catenin target, Axin-2. These finding suggest that cytoskeletal structure, which is subject to regulation by dynamic and static external mechanical factors, may impose a cytomolecular checkpoint at the level of LINC complexes to regulate  $\beta$ catenin access to the inner nucleus.

Consistent with the hypothesis that LINC participates in nuclear import of  $\beta$ catenin, depletion of Sun proteins also results in diminished association of  $\beta$ catenin with the nucleoskeleton. For endogenous  $\beta$ catenin, co-immunostaining of Nesprin-2 and  $\beta$ catenin corroborates that LINC complex guides  $\beta$ catenin localization: displacement of Nesprin-2 from the nuclear envelope reduced the  $\beta$ catenin localization to the nuclear surface. When

GFP- $\beta$ catenin was overexpressed, Sun 1/2 deletion slowed, but did not prevent  $\beta$ catenin nuclear entry, suggesting that the protein crowding caused by GFP- $\beta$ catenin overexpression might overcome LINC deficiency by increasing the probability of  $\beta$ catenin positioning at nuclear pores. NPCs are multi-component protein complexes that regulate many functions in cells (Kabachinski and Schwartz, 2015) and Sun-1 depletion has been shown to cause NPC clustering. (Liu et al., 2007). While it is possible that changes in NPC distribution and structure may contribute to delays in  $\beta$ catenin entry in Sun-1/2 depleted cells (Fig. 3f), this considerations was out of scope of the current study. Critically, LINC deficiency limited the ability of all  $\beta$ catenin stimuli - LIV, mechanical strain and pharmacologic - to first associate with the nucleoskeleton before trafficking into the soluble nuclear fraction. In contrast to depletion of Sun-1 and Sun-2, depletion of either Emerin or LaminA/C had no measurable effects on mechanically-induced  $\beta$ catenin association with nucleoskeleton. Together these findings indicate that LINC positioning of  $\beta$ catenin in the external nuclear envelope is a prerequisite for nuclear entry of  $\beta$ catenin.

Once inside the nucleus,  $\beta$ catenin can act as a transcription factor. While we did not address transcriptional outcomes in this study, both the nuclear membrane and Lamin A/C maintain dynamic interactions with chromatin (Czapiewski et al., 2016). Thus, increased association of  $\beta$ catenin with the nucleoskeleton, together with its previous disassociation from Nesprin-2, suggests that LINC may also regulate  $\beta$ catenin association with chromatin and access to target genes.

In summary, our data indicate that  $\beta$ catenin nuclear entry involves a rapid and reversible association with the insoluble nuclear fraction, opening new avenues important for understanding  $\beta$ catenin kinetics. Moreover, alterations in LINC-mediated connections interfere with  $\beta$ catenin's association with the nucleoskeleton, ultimately reducing nuclear transfer of  $\beta$ catenin nuclear. As such, mechanically induced adaptations of LINC complexes have the potential to augment the effectiveness of the Wnt pathway by improving  $\beta$ catenin nuclear trafficking in cells. As applied biophysics applications are gaining traction in tissue engineering and regenerative medicine to improve scaffold performance (Rando and Ambrosio, 2018), our findings may lead to more effective strategies to improve scaffold performance and MSC fate decisions.

## Materials and Methods

### Cell Culture, Pharmacological Reagents and antibodies

MSC were isolated from 8-10 wk male C57BL/6 mice were prepared after Peister et al (Peister et al., 2004). For phosphorylation measurements, seeding density was 10,000 cells/cm<sup>2</sup> and 3000 cells/cm<sup>2</sup> for immunostaining experiments. All groups were cultured for 48h before beginning experiments and were serum starved overnight in serum free medium. For transiently silencing specific genes, cells were transfected with gene-specific small interfering RNA (siRNA) or control siRNA (20 nM) using PepMute Plus transfection reagent (SignaGen Labs, Rockville, MD) according to manufacturer's instructions. PEGFP-C1- $\beta$ catenin (#16071) plasmid was purchased from Addgene. mdMSCs were transfected using 1 $\mu$ g DNA per 100,000 cells using LipoD293 transfection reagent (SignaGen Labs) according to manufacturer's instructions. Please see Table S3 for specific siRNA sequences



and Table S7 for reagent concentrations. Transfections and siRNA were applied 72h prior to Strain, LIV or SB415286. A complete list of all the reagents, DNA/RNAi sequences, antibodies and primers along with their final concentrations are provided in the supplementary appendix.

### **Application of LIV and Strain**

Vibrations were applied at peak magnitudes of 0.7g at 90Hz for 20min at room temperature. Uniform 2% equibiaxial strain was delivered at 10 cycles per minute for 20 min using the Flexcell FX-4000 system (Flexcell International, Hillsborough, NC). Controls were sham handled. Unless stated otherwise, both LIV and strain were applied twice for 20min separated by 2h rest period, a regimen we previously shown be effective in regulating  $\beta$ catenin signaling, cytoskeletal remodeling and MSC differentiation (Sen et al., 2011).

### **Isolation of Nucleoskeleton, soluble nuclear and nuclear envelope proteins**

Nucleoskeletal fraction was obtained by utilizing a modified version of previously published nuclear isolation protocol (Sen et al., 2011). Please see supplementary appendix for details.

### **Immunofluorescence, nuclear morphology and colocalization**

72h after the siRNA treatment against Sun-1 and Sun-2 proteins, cells were immunostained as previously described (Uzer et al., 2015). Nuclear morphology was extracted from Z-stack confocal 3D images, obtained and analyzed as previously described (Sen et al., 2017). Colocalization between Nesprin-2 and  $\beta$ catenin was assessed via ImageJ, please see supplementary appendix for details.

### **Protein and Gene Expression Quantification**

Protein quantification via Western Blot analyses and gene expression analyses were performed as previously described (Uzer et al., 2015).

### **Fluorescence recovery after photo bleaching**

PEGFP-C1- $\beta$ catenin transfected MSCs were imaged in a live chamber at 37°C and 5% CO<sub>2</sub> attached to a Zeiss LSM 710 confocal microscope. Images were taken using 40x objective lens. During imaging, nuclear region of interest was selected from images and ablated for 0.2s to bleach nuclear  $\beta$ catenin. Following the bleaching, GFP signal within the original region of interest was observed for 500sec with 0.2sec observation intervals. Recovery curves for both siCtrl and siSUN treated cells were constructed using Zen 2011 FRAP module and imported into Excel for data analysis.

### **Statistical analysis**

Results were presented as mean  $\pm$  SEM. Densitometry and other analyses were performed on at least three separate experiments. Normality was assessed via Kolmogorov-Smirnov test ( $\alpha=0.05$ ). Differences between groups were identified using un-paired t-test, Mann-Whitney U-test and by one-way analysis of variance (ANOVA) followed by Newman-Keuls post-hoc tests as indicated in figure legends. P-values of less than 0.05 were considered significant.

## Supplementary Material

Refer to Web version on PubMed Central for supplementary material.

## Acknowledgments

This study was supported by NIH AR056655 (JR), AR066616 (JR), EB014351 (JR), AR062097 (MS), P30DK056350 (MS), P20GM109095 (GU) and NSBRI PF04304 (GU) and NASA EPSCoR NNX15AK35A (GU).

Funding support: This study was supported by NIH AR056655 (JR), AR066616 (JR), EB014351 (JR), AR062097 (MS), P30DK056350 (MS), P20GM109095 (GU) and NSBRI PF04304 (GU) and NASA EPSCoR NNX15AK35A (GU).

## References

- Aberle H, Schwartz H, Kemler R. Cadherin-catenin complex: protein interactions and their implications for cadherin function. *J Cell Biochem.* 1996; 61:514–523. [PubMed: 8806074]
- Baron R, Kneissel M. WNT signaling in bone homeostasis and disease: from human mutations to treatments. *Nat Med.* 2013; 19:179–192. [PubMed: 23389618]
- Burridge K, Wittchen ES. The tension mounts: Stress fibers as force-generating mechanotransducers. *The Journal of Cell Biology.* 2013; 200:9–19. [PubMed: 23295347]
- Case N, Ma M, Sen B, Xie Z, Gross TS, Rubin J.  $\beta$ -Catenin Levels Influence Rapid Mechanical Responses in Osteoblasts. *Journal of Biological Chemistry.* 2008; 283:29196–29205. [PubMed: 18723514]
- Case N, Xie Z, Sen B, Styner M, Zou M, O’Conor C, Horowitz M, Rubin J. Mechanical activation of  $\beta$ -catenin regulates phenotype in adult murine marrow-derived mesenchymal stem cells. *Journal of Orthopaedic Research.* 2010; 28:1531–1538. [PubMed: 20872592]
- Cong F, Schweizer L, Chamorro M, Varmus H. Requirement for a Nuclear Function of  $\beta$ -Catenin in Wnt Signaling. *Molecular and Cellular Biology.* 2003; 23:8462–8470. [PubMed: 14612392]
- Cook PR. The nucleoskeleton: artefact, passive framework or active site? *Journal of cell science.* 1988; 90(Pt 1):1–6. [PubMed: 3058728]
- Crisp M, Liu Q, Roux K, Rattner JB, Shanahan C, Burke B, Stahl PD, Hodzic D. Coupling of the nucleus and cytoplasm: role of the LINC complex. *The Journal of Cell Biology.* 2006; 172:41–53. [PubMed: 16380439]
- Czapiewski R, Robson MI, Schirmer EC. Anchoring a Leviathan: How the Nuclear Membrane Tethers the Genome. *Frontiers in genetics.* 2016; 7:82. [PubMed: 27200088]
- Duong NT, Morris GE, Lam LT, Zhang Q, Sewry CA, Shanahan CM, Holt I. Nesprins: Tissue-Specific Expression of Epsilon and Other Short Isoforms. *PLoS ONE.* 2014; 9:e94380. [PubMed: 24718612]
- Graham DM, Andersen T, Sharek L, Uzer G, Rothenberg K, Hoffman BD, Rubin J, Bolland M, Bear JE, Burridge K. Eucleated cells reveal differential roles of the nucleus in cell migration, polarity, and mechanotransduction. *J Cell Biol.* 2018; 217:895–914. [PubMed: 29351995]
- Gruenbaum Y, Margalit A, Goldman RD, Shumaker DK, Wilson KL. The nuclear lamina comes of age. *Nat Rev Mol Cell Biol.* 2005; 6:21–31. [PubMed: 15688064]
- Hernandez L, Roux KJ, Wong ESM, Mounkes LC, Mutalif R, Navasankari R, Rai B, Cool S, Jeong JW, Wang H, Lee HS, Kozlov S, Grunert M, Keeble T, Jones CM, Meta MD, Young SG, Daar IO, Burke B, Perantoni AO, Stewart CL. Functional Coupling between the Extracellular Matrix and Nuclear Lamina by Wnt Signaling in Progeria. *Developmental Cell.* 2010; 19:413–425. [PubMed: 20833363]
- Jorgens DM, Inman JL, Wojcik M, Robertson C, Palsdottir H, Tsai WT, Huang H, Bruni-Cardoso A, Lopez CS, Bissell MJ, Xu K, Auer M. Deep nuclear invaginations linked to cytoskeletal filaments: Integrated bioimaging of epithelial cells in 3D culture. *Journal of cell science.* 2016
- Kabachinski G, Schwartz TU. The nuclear pore complex – structure and function at a glance. *Journal of cell science.* 2015; 128:423–429. [PubMed: 26046137]

- Koike M, Kose S, Furuta M, Taniguchi N, Yokoya F, Yoneda Y, Imamoto N.  $\beta$ -Catenin Shows an Overlapping Sequence Requirement but Distinct Molecular Interactions for Its Bidirectional Passage through Nuclear Pores. *Journal of Biological Chemistry*. 2004; 279:34038–34047. [PubMed: 15173161]
- Leung JY, Kolligs FT, Wu R, Zhai Y, Kuick R, Hanash S, Cho KR, Fearon ER. Activation of AXIN2 Expression by  $\beta$ -Catenin-T Cell Factor: a Feedback Repressor Pathway Regulating Wnt Signaling. *Journal of Biological Chemistry*. 2002; 277:21657–21665. [PubMed: 11940574]
- Liu Q, Pante N, Misteli T, Elsagga M, Crisp M, Hodzic D, Burke B, Roux KJ. Functional association of Sun1 with nuclear pore complexes. *J Cell Biol*. 2007; 178:785–798. [PubMed: 17724119]
- Lu W, Schneider M, Neumann S, Jaeger VM, Taranum S, Munck M, Cartwright S, Richardson C, Carthew J, Noh K, Goldberg M, Noegel A, Karakesisoglou I. Nesprin interchain associations control nuclear size. *Cellular and Molecular Life Sciences*. 2012; 69:3493–3509. [PubMed: 22653047]
- Markiewicz E, Tilgner K, Barker N, van de Wetering M, Clevers H, Dorobek M, Hausmanowa-Petrusewicz I, Ramaekers FCS, Broers JLV, Blankesteyn WM, Salpingidou G, Wilson RG, Ellis JA, Hutchison CJ. The inner nuclear membrane protein Emerin regulates [beta]-catenin activity by restricting its accumulation in the nucleus. *EMBO J*. 2006; 25:3275–3285. [PubMed: 16858403]
- Meyer MB, Benkusky NA, Sen B, Rubin J, Pike JW. Epigenetic Plasticity Drives Adipogenic and Osteogenic Differentiation of Marrow-derived Mesenchymal Stem Cells. *Journal of Biological Chemistry*. 2016; 291:17829–17847. [PubMed: 27402842]
- Neumann S, Schneider M, Daugherty RL, Gottardi CJ, Eming SA, Beijer A, Noegel AA, Karakesisoglou I. Nesprin-2 Interacts with  $\alpha$ -Catenin and Regulates Wnt Signaling at the Nuclear Envelope. *Journal of Biological Chemistry*. 2010; 285:34932–34938. [PubMed: 20801886]
- Peister A, Mellad JA, Larson BL, Hall BM, Gibson LF, Prockop DJ. Adult stem cells from bone marrow (MSCs) isolated from different strains of inbred mice vary in surface epitopes, rates of proliferation, and differentiation potential. 2004
- Rando TA, Ambrosio F. Regenerative Rehabilitation: Applied Biophysics Meets Stem Cell Therapeutics. *Cell Stem Cell*. 2018; 22:306–309. [PubMed: 29499150]
- Robinson JA, Chatterjee-Kishore M, Yaworsky PJ, Cullen DM, Zhao W, Li C, Kharode Y, Sauter L, Babij P, Brown EL, Hill AA, Akhter MP, Johnson ML, Recker RR, Komm BS, Bex FJ. Wnt/ $\beta$ -Catenin Signaling Is a Normal Physiological Response to Mechanical Loading in Bone. *Journal of Biological Chemistry*. 2006; 281:31720–31728. [PubMed: 16908522]
- Sen B, Styner M, Xie Z, Case N, Rubin CT, Rubin J. Mechanical Loading Regulates NFATc1 and  $\beta$ -Catenin Signaling through a GSK3 $\beta$  Control Node. *Journal of Biological Chemistry*. 2009; 284:34607–34617. [PubMed: 19840939]
- Sen B, Uzer G, Samsonraj RM, Xie Z, McGrath C, Styner M, Dudakovic A, van Wijnen AJ, Rubin J. Intranuclear Actin Structure Modulates Mesenchymal Stem Cell Differentiation. *Stem Cells*. 2017; 35:1624–1635. [PubMed: 28371128]
- Sen B, Xie Z, Case N, Styner M, Rubin CT, Rubin J. Mechanical signal influence on mesenchymal stem cell fate is enhanced by incorporation of refractory periods into the loading regimen. *Journal of biomechanics*. 2011; 44:593–599. [PubMed: 21130997]
- Sen B, Xie ZH, Case N, Ma MY, Rubin C, Rubin J. Mechanical Strain Inhibits Adipogenesis in Mesenchymal Stem Cells by Stimulating a Durable beta-Catenin Signal. *Endocrinology*. 2008; 149:6065–6075. [PubMed: 18687779]
- Sharma M, Jamieson C, Johnson M, Molloy MP, Henderson BR. Specific Armadillo Repeat Sequences Facilitate  $\beta$ -Catenin Nuclear Transport in Live Cells via Direct Binding to Nucleoporins Nup62, Nup153, and RanBP2/Nup358. *Journal of Biological Chemistry*. 2012; 287:819–831. [PubMed: 22110128]
- Simon DN, Wilson KL. The nucleoskeleton as a genome-associated dynamic 'network of networks'. *Nat Rev Mol Cell Biol*. 2011; 12:695–708. [PubMed: 21971041]
- Tajik A, Zhang Y, Wei F, Sun J, Jia Q, Zhou W, Singh R, Khanna N, Belmont AS, Wang N. Transcription upregulation via force-induced direct stretching of chromatin. *Nature materials*. 2016; 15:1287–1296. [PubMed: 27548707]

- Thompson WR, Guilluy C, Xie Z, Sen B, Brobst KE, Yen SS, Uzer G, Styner M, Case N, Burrige K, Rubin J. Mechanically Activated Fyn Utilizes mTORC2 to Regulate RhoA and Adipogenesis in Mesenchymal Stem Cells. *STEM CELLS*. 2013; 31:2528–2537. [PubMed: 23836527]
- Tolwinski NS, Wieschaus E. A nuclear function for armadillo/beta-catenin. *PLoS biology*. 2004; 2:E95. [PubMed: 15024404]
- Uzer G, Pongkitwitoon S, Ete Chan M, Judex S. Vibration induced osteogenic commitment of mesenchymal stem cells is enhanced by cytoskeletal remodeling but not fluid shear. *Journal of biomechanics*. 2013; 46:2296–2302. [PubMed: 23870506]
- Uzer G, Rubin CT, Rubin J. Cell Mechanosensitivity Is Enabled by the LINC Nuclear Complex. *Current Molecular Biology Reports*. 2016; 2:36–47. [PubMed: 27326387]
- Uzer G, Thompson WR, Sen B, Xie Z, Yen SS, Miller S, Bas G, Styner M, Rubin CT, Judex S, Burrige K, Rubin J. Cell Mechanosensitivity to Extremely Low-Magnitude Signals Is Enabled by a LINCed Nucleus. *STEM CELLS*. 2015; 33:2063–2076. [PubMed: 25787126]
- Zhang Q, Minaisah RM, Ferraro E, Li C, Porter LJ, Zhou C, Gao F, Zhang J, Rajgor D, Autore F, Shanahan CM, Warren DT. N-terminal nesprin-2 variants regulate beta- catenin signalling. *Experimental cell research*. 2016; 345:168–179. [PubMed: 27321956]

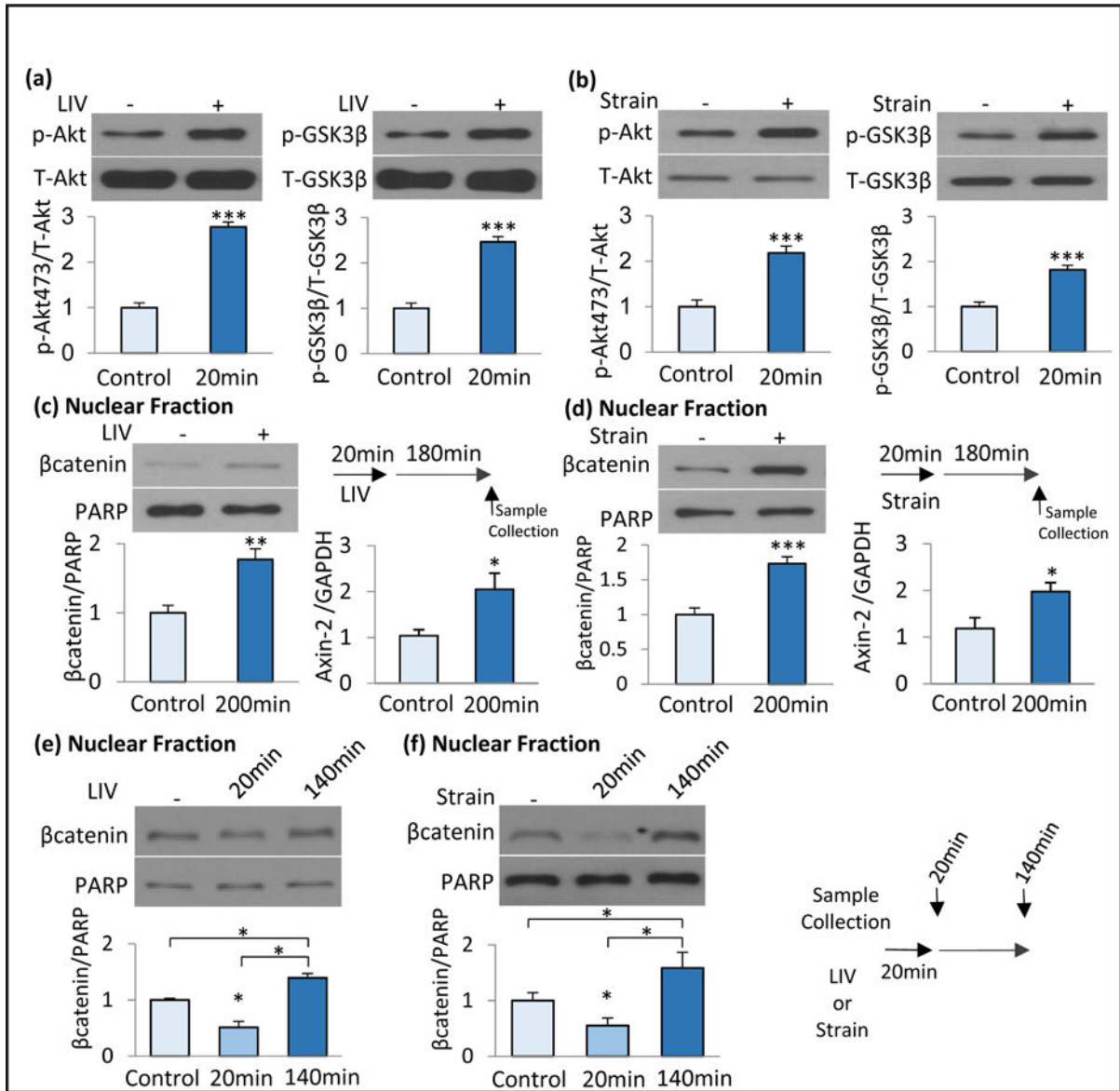


**Figure 1. Mechanical inactivation of GSK3β leads to a non-monotonic increase of nuclear βcatenin**

**a)** Application of LIV (0.7g, 90Hz, 20min) increased p-Akt (277%,  $p < 0.001$ ,  $n = 3$ ) and p-GSK3β (246%,  $p < 0.001$ ,  $n = 3$ ). **b)** Application of strain (2%, 0.17Hz, 20min) increased in p-Akt (218%,  $p < 0.001$ ,  $n = 3$ ) and p-GSK3β (181%,  $p < 0.001$ ,  $n = 3$ ). **c)** Three hours post-LIV, both βcatenin in the soluble nuclear fractions (177%,  $p < 0.01$ ,  $n = 6$ ) and Axin-2 gene expression (205%,  $p < 0.05$ ,  $n = 6$ ) were increased. **d)** Three hours post-strain, both βcatenin in the soluble nuclear fractions (173%,  $p < 0.001$ ,  $n = 6$ ) and Axin-2 gene expression (198%,  $p < 0.05$ ,  $n = 6$ ) were increased. **e)** MSCs were subjected to a single LIV bout and samples were collected immediately (20min) or 120min after ( $n = 3$ ). LIV acutely decreased βcatenin in the soluble nuclear fraction to 49% ( $p < 0.05$ ), 120min later βcatenin was 140% of non-LIV control ( $p < 0.05$ ). **f)** MSCs were subjected to a single strain bout and samples were collected immediately (20min) or 120min after ( $n = 3$ ). Strain acutely decreased

$\beta$ catenin in the soluble nuclear fraction to 45% ( $p<0.05$ ), 120min later  $\beta$ catenin was 159% of non-strain control. Group comparisons were made using unpaired T-test (Figure 1a-d) and One-way ANOVA followed by a Newman-Keuls post-hoc test (Fig.1e-f). \*  $p<0.05$ , \*\*  $p<0.01$ , \*\*\*  $p<0.001$ , against control and each other.

Author Manuscript

Author Manuscript

Author Manuscript

Author Manuscript

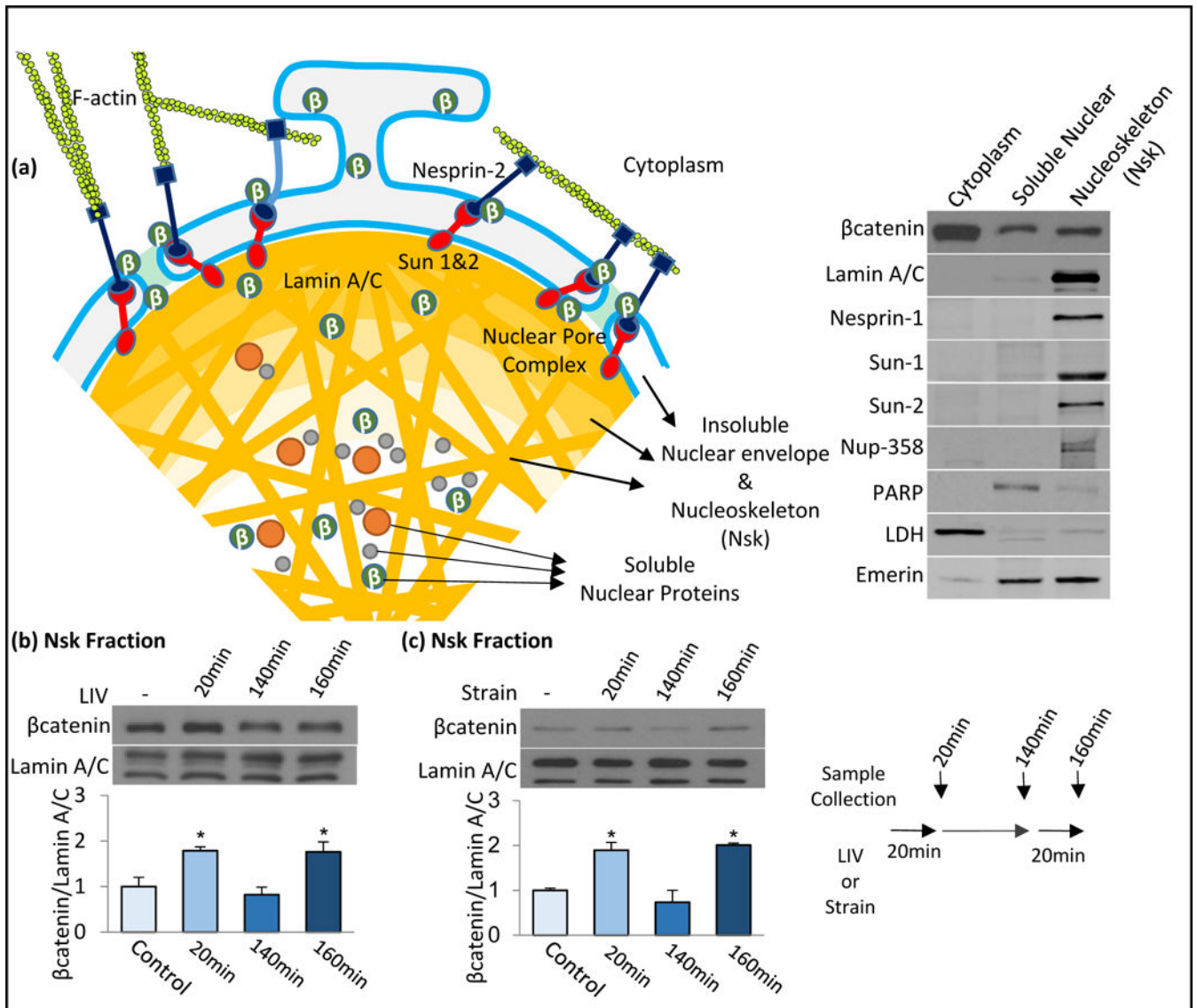


**Figure 2. Mechanical signals cause rapid and transient βcatenin association with nucleoskeleton**

**a)** Schematic of nuclear envelope and nucleoskeleton connected to the F-actin cytoskeleton via LINC complexes (Nesprin-2 and Sun-1&2). At basal state, βcatenin can be found in both cytoplasm, nuclear envelope and nuclear fractions. We isolated the insoluble nucleoskeletal fraction (Nsk) enriched with Nuclear envelope proteins, LaminA/C and Nucleoporins to probe possible interactions of βcatenin with nucleoskeletal and nuclear envelope scaffold. **b)** MSCs were subjected to a single LIV bout (0.7g, 90Hz, 20min) and samples were collected immediately (20min) or 120min after. A third group was subjected to an initial LIV bout was subjected to a second LIV bout for 20min and collected immediately after LIV (160min total). Immediately after first LIV bout, βcatenin-Nsk association was increased to 178% ( $p < 0.05$ ,  $n = 3$ ) which returned to baseline after 120min (82%, NS,  $n = 3$ ). A second LIV bout elevated βcatenin-Nsk association to 176% ( $p < 0.05$ ,  $n = 3$ ) of non-LIV control. **c)** MSCs were subjected to a single strain bout (2%, 0.17Hz, 20min) and samples were collected immediately (20min) or 120min after. A third group was subjected to initial strain bout was

subjected to a second strain bout for 20min and collected immediately after strain (160min total). Immediately after first strain bout,  $\beta$ catenin-Nsk association was increased to 189% ( $p < 0.05$ ,  $n=3$ ) which returned to baseline 120min after (73%, NS). A second strain bout elevated  $\beta$ catenin-Nsk association to 200% of non-strain control. Group comparisons were made using One-way ANOVA followed by a Newman-Keuls post-hoc test (Fig.2b-c). ( $p < 0.05$ ,  $n=3$ ). \*  $p < 0.05$ , \*\*  $p < 0.01$ , \*\*\*  $p < 0.001$ , against control and each other.

Author Manuscript

Author Manuscript

Author Manuscript

Author Manuscript



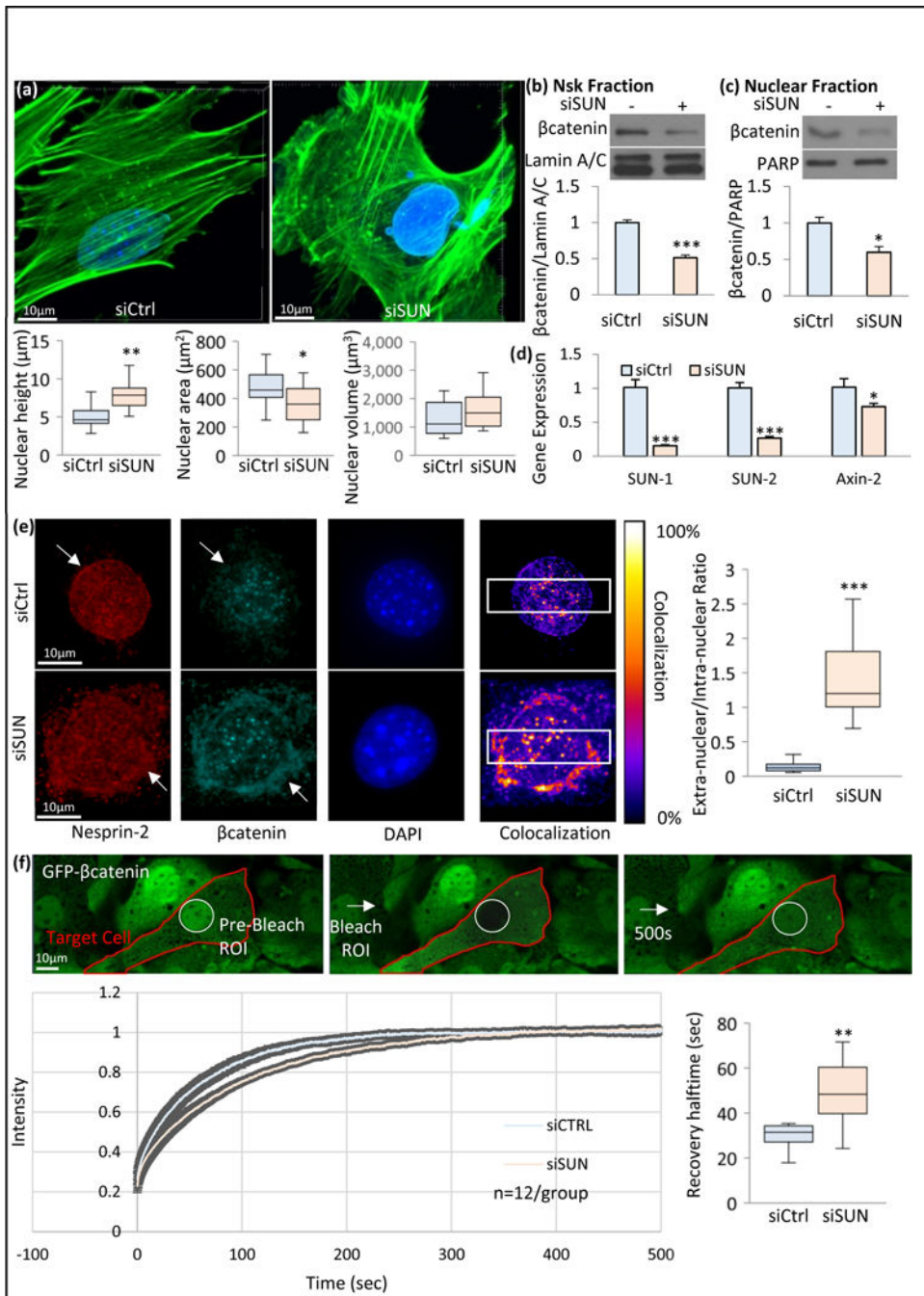


**Figure 3. Co-depletion of LINC elements Sun-1 and Sun-2 disrupts  $\beta$ catenin-nucleoskeleton association and  $\beta$ catenin in the soluble nuclear fraction**

**a)** Nesprin anchoring LINC elements Sun-1 and Sun-2 were co-depleted via siRNAs against Sun-1 and Sun-2 (siSUN) and compared to non-targeting siRNA (siCtrl). Nuclear morphology was quantified via confocal stacks in both siCtrl and siSUN treated MSCs. F-actin was visualized by phalloidin and DNA was visualized via DAPI. Compared with siCtrl, siSUN group showed a 57% increase in nuclear height ( $p < 0.01$ ,  $n = 12$ ) and a 23% decrease in nuclear area 23% ( $p < 0.05$ ,  $n = 12$ ) but no change in nuclear volume was observed.

**b)** Comparing  $\beta$ catenin compartmentalization with siCtrl, siSUN treatment decreased  $\beta$ catenin-Nsk association to 51% ( $p < 0.001$ ,  $n = 4$ ) and **c)** nuclear  $\beta$ catenin levels to 59% ( $p < 0.05$ ,  $n = 4$ ). **d)** Axin-2 gene expression was also decreased by 29% ( $p < 0.05$ ,  $n = 6$ ) in siSUN treatment when compared to siCtrl. **e)** Nesprin-2 and  $\beta$ catenin immunostaining were compared between siCtrl and siSUN treated cells. In siSUN treated cells, both Nesprin-2 and  $\beta$ catenin were partly localized in extranuclear region, outside of the DAPI stained nucleus, while in SiCtrl cells both Nesprin-2 and  $\beta$ catenin were primarily intranuclear (white arrows). Colocalization between Nesprin-2 and  $\beta$ catenin was detectable in both siCtrl and siSUN treated cells. To quantify the differences, colocalization within a region of interest (white box) was plotted across the horizontal axis (Fig.S1) for both groups. Quantification of extranuclear to intranuclear ratio of Nesprin-2 and  $\beta$ catenin within this region of interest was compared between siSUN and siCtrl groups ( $p < 0.001$ ,  $n = 12$ ). **f)** Nuclear region of interest in GFP- $\beta$ catenin expressing MSCs were ablated and fluorescence recovery after photo bleaching (FRAP) was measured. siSUN treated MSCs showed a 51% recovery delay ( $p < 0.01$ ,  $n = 12$ ) as measured by FRAP, indicating a slower  $\beta$ catenin entry. Group comparisons were made using unpaired T-test (Figure 3b-d) and Mann-Whitney U-test (Fig. 3a, 3e & 3f). \*  $p < 0.05$ , \*\*  $p < 0.01$ , \*\*\*  $p < 0.001$ , against control.

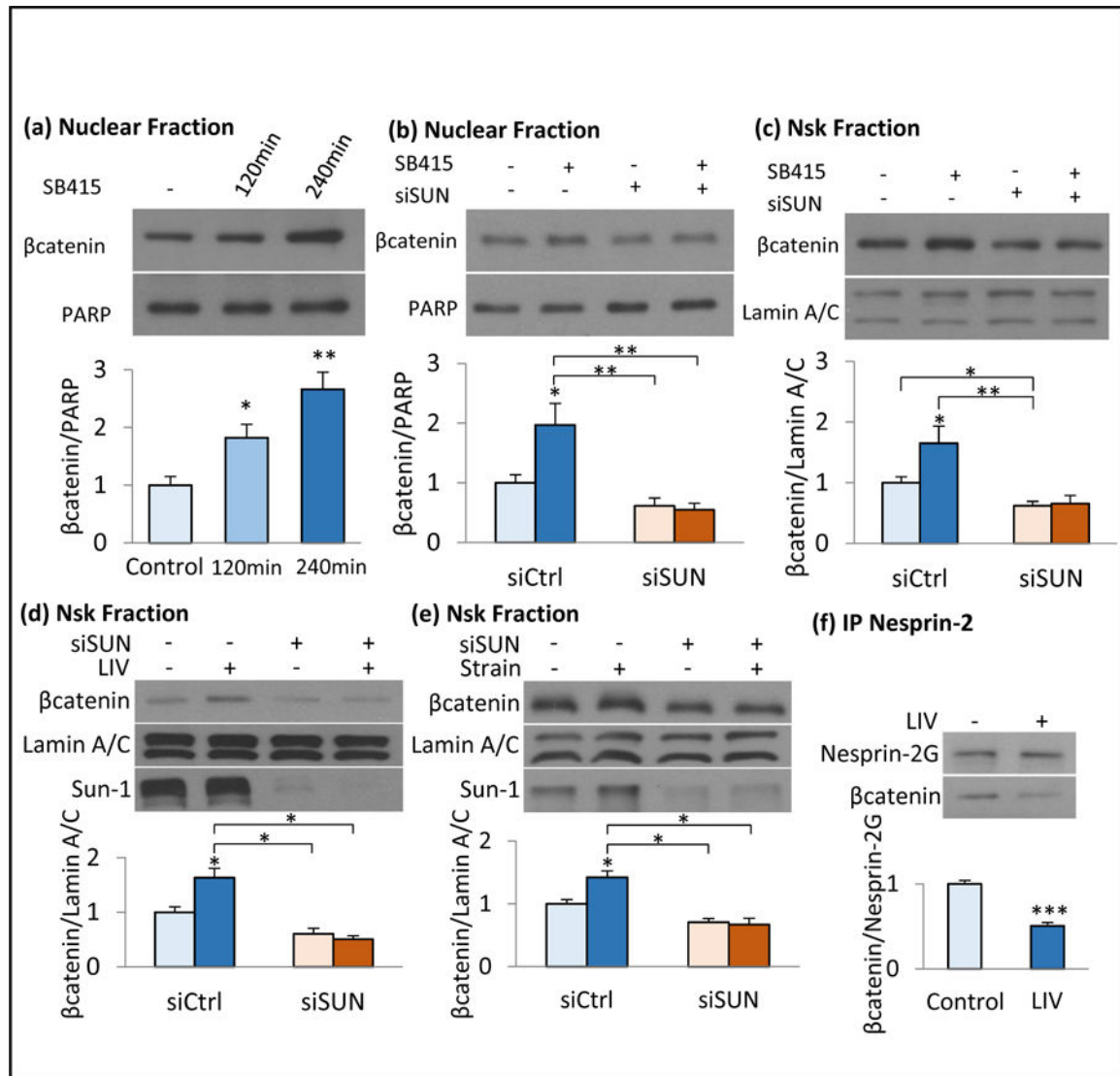


**Figure 4. LINC elements Sun-1 and Sun-2 are required for βcatenin nuclear entry and βcatenin-nucleoskeleton association**

**a)** SB415 steadily increased the nuclear βcatenin to 182% ( $p < 0.05$ ) and 266% ( $p < 0.01$ ) of baseline levels at 120min and 240min, respectively ( $n = 4$ ). **b)** Soluble nuclear βcatenin was measured 180min after of SB415 treatment. Compared to siCtrl, siSUN treated MSCs decreased both basal and SB415 induced nuclear βcatenin ( $p < 0.05$ ,  $n = 3$ ). **c)** βcatenin-Nsk association was increased to 165% ( $p < 0.05$ ,  $n = 3$ ) in SB415 treated siCtrl cells but siSUN decreased basal βcatenin-Nsk association in both DMSO (62%,  $p < 0.01$ ,  $n = 3$ ) and SB415 (65%,  $p < 0.05$ ,  $n = 3$ ), treated MSCs. **d)** siSUN decreased basal Nsk-bound βcatenin to 60% ( $p < 0.05$ ,  $n = 3$ ) and LIV induced βcatenin-Nsk association was inhibited in siSUN treated MSCs ( $p < 0.05$ ,  $n = 3$ ). **e)** Similarly, siSUN decreased both basal Nsk-bound βcatenin to 70% ( $p < 0.05$ ,  $n = 3$ ) and inhibited the strain induced βcatenin-Nsk association ( $p < 0.05$ ,  $n = 3$ ). **f)** Nesprin-2 was immunoprecipitated immediately following LIV and probed against βcatenin. LIV decreased Nesprin-2-βcatenin association 50% ( $p < 0.001$ ,  $n = 4$ ). Please see Fig.S4 for a more detailed blot. Group comparisons were made using unpaired T-test (Figure 4f) and

One-way ANOVA followed by a Newman-Keuls post-hoc test (Fig.4a-e). \*  $p < 0.05$ , \*\*  $p < 0.01$ , \*\*\*  $p < 0.001$ , against control and each other.

Author Manuscript

Author Manuscript

Author Manuscript

Author Manuscript